

Article

Preparation of Slow-Release Potassium Persulfate Microcapsules and Application in Degradation of PAH-Contaminated Soil

Hao Wu ^{1,2}, Yuting Yang ³, Lina Sun ^{1,*}, Yinggang Wang ^{1,*}, Hui Wang ^{3,4} and Xiaoxu Wang ³¹ Environment College, Shenyang University, Shenyang 110044, China; zhu13mao@163.com² Engineering Research Center of Groundwater Pollution Control and Remediation, Ministry of Education of China, Beijing Normal University, Beijing 100091, China³ Key Laboratory of Regional Environmental and Eco-Remediation, Ministry of Education, Shenyang University, Shenyang 110044, China; 13940454983@163.com (Y.Y.); huiwang425@126.com (H.W.); 13840554151@163.com (X.W.)⁴ Northeast Geological S&T Innovation Center of China Geological Survey, Shenyang 110000, China

* Correspondence: ericwh@126.com (L.S.); yinggangwang@syu.edu.cn (Y.W.)

Abstract: Due to potassium persulfate's excessive reaction speed and severe impact on the soil environment, slowing down the reaction rate and reducing its environmental impact is an important but challenging matter. Hence, microencapsulation technology was taken to modify potassium persulfate, and potassium persulfate microcapsules were used to remediate the PAHs-contaminated soil. The results of XRD and an infrared spectrum identified that the core material (potassium persulfate) exists after being encapsulated by the wall material (stearic acid), and there was no chemical reaction between the core material and wall material. The results of the sustained release effect and kinetic equation showed that the release rate of the potassium persulfate microcapsules was close to 60% after 48 h, and it had a good sustained-release effect compared with previous studies. The results of the radical probe revealed that the free radicals produced from potassium persulfate microcapsules activated by Fe²⁺ were the main reasons for the degradation of PAHs, and SO₄⁻· played the most important major role in the degradation of PAHs, followed by ·OH, and the reducing substances also played an auxiliary role. The results also suggested that potassium persulfate microcapsules not only degraded PAHs in soil (53.6% after 72 h) but also had fewer negative effects on the environment, and they even promoted the growth and development of microorganisms and increased the germination rate of seeds due to the slow-release effect of the microcapsules. This work reveals the degradation mechanism of potassium persulfate microcapsules and provides a new amendment of potassium persulfate in the remediation of PAHs-contaminated soil.

Keywords: potassium persulfate; PAH contaminated soil; slow release; microcapsule

Citation: Wu, H.; Yang, Y.; Sun, L.; Wang, Y.; Wang, H.; Wang, X. Preparation of Slow-Release Potassium Persulfate Microcapsules and Application in Degradation of PAH-Contaminated Soil. *Water* **2024**, *16*, 3045. <https://doi.org/10.3390/w16213045>

Academic Editor: Didier Orange

Received: 20 September 2024

Revised: 18 October 2024

Accepted: 19 October 2024

Published: 24 October 2024



Copyright: © 2024 by the authors. Licensee MDPI, Basel, Switzerland. This article is an open access article distributed under the terms and conditions of the Creative Commons Attribution (CC BY) license (<https://creativecommons.org/licenses/by/4.0/>).

1. Introduction

As a typical advanced oxidation technology, potassium persulfate (K₂S₂O₈) is known for its good remediation effect and fast repair speed to organic pollutants as well as its good stability, strong oxidation, and suitable water solubility (50 g/L, 20 °C) [1]. Sulfate-free radicals (SO₄⁻·, E₀ = 2.6 V) and hydroxyl free radicals (·OH, E₀ = 2.8 V), which have strong oxidation, would be generated by potassium persulfate after activation [2], and potassium persulfate has been used to remedy PAHs-contaminated soil [3–5]. However, the reaction rate of potassium persulfate is usually relatively fast; meanwhile, the repair process of potassium persulfate is an exothermic reaction, and the redox condition also changed significantly during the reaction process, which would affect the soil characteristics. Therefore, the utilization rate of potassium persulfate is usually low [6], and slowing down the reaction rate is essential. Microencapsulation technology is an implementation for controlled slow release using natural or synthetic membrane-forming materials to embed solid, liquid, or gaseous cores, and it has been widely used in some fields, such as food,

medicine, pesticide, fertilizer, oil extraction, etc. [7–11]. So, microencapsulation technology has strong application potential in soil remediation by potassium persulfate to slow down the reaction rate and reduce the environmental impact.

Due to potential carcinogenic human and environmental impacts, polycyclic aromatic hydrocarbons (PAHs) have been listed as priority pollutants [12–14], and they are widely studied in various environmental media [3–5,15,16]. Once PAHs enter into soil, it is easy to sorb onto fine-grained soil particles, and it exists in the soil for a long time due to its low aqueous solubility, semi-volatility, persistence, and stability [17–19]. Meanwhile, PAHs could alter soil microorganisms and even cause harm to mammalian health through the food chain [20–23]. Bioremediation has been used to cost-effectively remediate PAHs soils without causing secondary pollution [15,16,24–26], but the remediation efficiency is relatively low compared with chemical remediation. Physical and chemical remediation methods could quickly remedy organic-contaminated soil [27,28], but the microbial community and chemical soil quality could be compromised during repair, and they are unsuitable for remediating agricultural soils and subsequent bioremediation [29]. Therefore, an efficient and ecologically friendly soil remediation method is required.

Based on the above analysis, we fully combined the advantages of potassium persulfate and microcapsules to prepare potassium persulfate microcapsules, and we applied them to remediate the PAHs-contaminated soil. The purposes of this study were to (1) characterize the potassium persulfate microcapsules; (2) reveal the sustained release behavior of potassium persulfate from the microcapsules; (3) elucidate the degradation effect and mechanism of PAH contaminated soil by potassium persulfate microcapsules; and (4) evaluate the effects on the environment after being degraded by microcapsules. In this study, a soil remediation method with broad application prospects was proposed, and it was efficient and ecologically friendly. Compared to traditional methods, the potassium persulfate microcapsule had less impact on the soil environment and soil microorganisms, and it was beneficial for subsequent bioremediation.

2. Materials and Methods

2.1. Reagent

Potassium persulfate ($K_2S_2O_8$) used in the experiment was purchased from Chinese Medicine, and stearic acid ($C_{18}H_{36}O_2$) was purchased from Beijing Merida. The analytically pure and chromatographically pure solvents used in the experiment were purchased from Sinopharm Chemical Reagent Co., Ltd. (Shanghai, China). The mixture stock standard solutions of U.S. EPA's Sixteen PAH Priority Pollutants was purchased from AccuStandard (New Haven, CT, USA), and it was used in this study. A high-performance liquid chromatography (HPLC, Agilent 1100) was used to analyze PAHs. Field emission scanning electron microscope and energy-dispersive spectrometer (SEM, s4800, Hitachi, Tokyo, Japan) and X-ray powder polycrystalline diffraction (XRD, D8 advance, Brooke, Billerica, MA, USA) were used to characterize the potassium persulfate microcapsules.

2.2. Preparation and Characterization of Potassium Persulfate Microcapsule

Due to its high solubility and ability to easily decompose at high temperatures, potassium persulfate microcapsules needed to be prepared in the oil phase, and the temperature was below 35 °C. First, 15 g stearic acid was put in a 100 mL beaker, and 50 mL anhydrous ethanol was added. It was stirred until it was well dissolved with magnetic force at 55 °C and 3000 r/min, and then 3 g polyethylene glycol was added to promote the package of potassium persulfate microcapsules. Then, potassium persulfate and an equal amount of bentonite were added, and the potassium persulfate microcapsule was vacuum-dried. Three different potassium persulfate microcapsules, in which the mass ratio of potassium persulfate and stearic acid was 1:1, 1:2, and 1:3, were prepared in this study, and the additive amount of potassium persulfate was 15 g, 10 g, and 5 g, respectively.

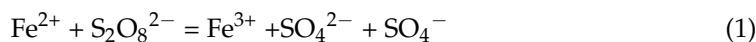
X-ray powder polycrystalline diffraction (XRD, D8 advance, Brooke) was used to analyze the structure of potassium persulfate microcapsules, and field emission scanning

electron microscope and energy-dispersive spectrometer (SEM, s4800, Hitachi) were used to observe the morphology of potassium persulfate microcapsules.

2.3. Experimental Design

The soil used in this study was sampled from the surface of the campus of Shenyang University, and it was a silty clay with the following composition: 28.13% clay, 70.63% silt, and 1.24% sand. Soil pH ranged from 6.88 to 7.15, and the organic matter content in soil was 5.46%, which was determined by the potassium dichromate outside heating method [17]. The mixture stock standard solutions of U.S. EPA's Sixteen PAH Priority Pollutants were added into the soil. The PAHs-contaminated soil was reserved after aging and storing in the dark for one year, and the pot experiment was carried out in the laboratory.

First, 1:2 potassium persulfate microcapsules were used to degrade PAHs-contaminated soil, and Fe^{2+} was added as an activator with a mass ratio of 1:10 of microcapsules. The chemical equations of the persulfate activation process are shown in equations 1 and 2 [30,31]. First, 0.1 g microcapsules were added in 25 g of polluted soil, and triplicates of each treatment were conducted. Soil samples were taken at intervals for a certain time (0 h, 1 h, 2 h, 4 h, 8 h, 12 h, 24 h, 48 h, and 72 h); the samples were air-dried, foreign matter was removed (e.g., rocks, plastic waste, and leaves), and then they were ground and sieved by a 60-mesh screen to obtain homogeneous samples.



PAHs in the samples were extracted by an accelerated solvent extractor (Dionex ASE300), and 1:1 (*v:v*) acetone/hexane was used as an extracting solution [32]. The silica gel column chromatography was used to purify the extractant solution [33]; then, it was evaporated and dissolved in 1 mL of acetonitrile (HPLC grade). At last, a high-performance liquid chromatography (HPLC 1100, Agilent, Santa Clara, CA, USA) with UV and a fluorescence detector were used to analyze the PAHs as the method of previous studies [34–36]. Recovery rates were 80.3–96.5%.

2.4. Degradation Mechanisms Analysis

Radical probe compounds are substances that only react with certain free radicals but do not react with other free radicals, oxidants, and pollutants. Usually, the persulfate after being activated produced free radicals, including $\text{SO}_4^{\cdot -}$, $\cdot\text{OH}$, and other free radicals, even reducing substances, and that was the important mechanism of persulfate degradation of pollutants [23,37]. Ethanol is usually used as the quencher of $\text{SO}_4^{\cdot -}$ and $\cdot\text{OH}$ due to the high quenching rate constant of $\text{SO}_4^{\cdot -}$ and $\cdot\text{OH}$ [38,39]. The reaction rate of nitrobenzene (NB) with $\cdot\text{OH}$ is 3 orders of magnitude higher than that of $\text{SO}_4^{\cdot -}$, so it can be used as a probe compound to compare between $\cdot\text{OH}$ and $\text{SO}_4^{\cdot -}$ [40,41]. Meanwhile, hexachloroethane (HCA) easily reacts with reducing substances (mainly including organic matter and low-priced metals in soil, including Fe^{3+} , Mn^{4+}), and it can be detected whether reducing substances participate in the reaction [42]. Therefore, ethanol, nitrobenzene, and hexachloromethane were selected as radical probe compounds, and they were used to determine the reaction mechanism in this study.

2.5. Data Analysis

The results of all indices represent the mean of triplicate samples. Excel 2020 and Origin9.0 were used to analyze data, generate figures, and perform curve fitting. *t*-tests were used to compare the results from each treatment, and a probability (P) of 0.05 was used to show statistical significance. Low-ring PAHs were the 2-ring PAHs and 3-ring PAHs, such as naphthalene, acenaphthylene, phenanthrene, and so on. High-ring PAHs were the 4-ring PAHs, 5-ring PAHs, and 6-ring PAHs, such as benz[a]anthracene, dibenz[a,h]anthracene, and so on.

3. Results and Discussions

3.1. Characterization of Potassium Persulfate Microcapsule

To analyze the changes in crystalline structure before and after the encapsulation of different proportions of microcapsules and judge whether stearic acid has successfully encapsulated potassium persulfate, the microcapsules and potassium persulfate were characterized by X-ray diffraction (XRD), and XRD patterns of potassium persulfate and microcapsules with three different proportions are shown in Figure 1. The results showed that potassium persulfate has a strong diffraction peak at $2\theta = 27.574^\circ$, which is the characteristic diffraction peak of potassium persulfate. The strong diffraction peaks of 1:1 microcapsules at $2\theta = 27.568^\circ$, 1:2 microcapsules at $2\theta = 27.574^\circ$, and 1:3 microcapsules at $2\theta = 27.521^\circ$ appeared in the same position as the absorption peaks of potassium persulfate, and it meant that the activity of potassium persulfate still existed and the crystal structure did not change. A new very low-intensity diffraction peak appeared in the microcapsules. The reasons may be that during the preparation of potassium persulfate microcapsules, such as the encapsulation and breakage of potassium persulfate, the morphology of potassium persulfate crystals changed [43], so there were differences in the detection process. Therefore, according to the XRD patterns of microcapsules, it is preliminarily determined that the potassium persulfate still exists after being encapsulated by stearic acid, and the potassium persulfate microcapsule could be used as an oxidant in the remediation of environmental pollution as potassium persulfate.

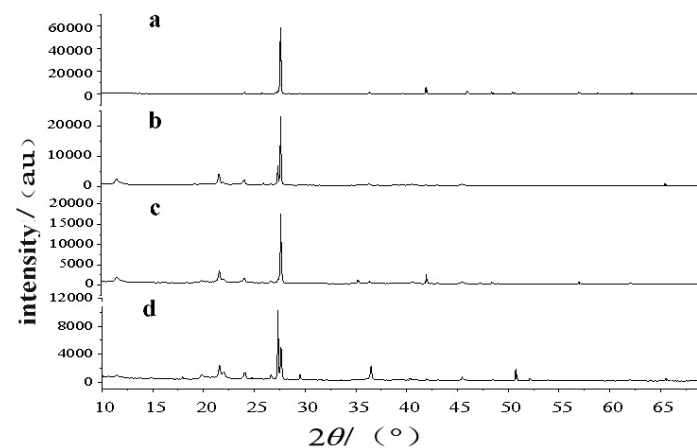


Figure 1. XRD patterns before and after microencapsulation of potassium persulfate. (a) Potassium persulfate before microencapsulation, (b) 1:3 microcapsules, (c) 1:2 microcapsules, and (d) 1:1 microcapsules.

The infrared spectrum results of stearic acid and potassium persulfate microcapsules are shown in Figure 2. For stearic acid, no absorption peak was at more than 3000 cm^{-1} , which meant there was only saturated C-H and no unsaturated C-H. At 1701 cm^{-1} , there was a stretching vibration peak of -C=O with the -COOH group, and at 1431 cm^{-1} , there was an in-plane bending vibration of -CH_3 and -CH_2 [44,45]. The absorption peak at 720 cm^{-1} was due to the in-plane oscillation of -CH_2 , which was consistent with the structure of stearic acid [46]. The characteristic absorption peaks at 2917 cm^{-1} , 1701 cm^{-1} , 1431 cm^{-1} , and 720 cm^{-1} are found in the 1:2 microcapsule, which are the same as those of stearic acid. It can be seen that the characteristic absorption peak of stearic acid has not been destroyed. It suggested that there was no chemical reaction between the core material and wall material, when potassium persulfate was wrapped by stearic acid [47,48]. The surface characterization of 1:2 microcapsules was observed by SEM, and the results are shown in Figure 3. The microcapsules were observed at $2\text{ }\mu\text{m}$ and $10\text{ }\mu\text{m}$, respectively. Before sustained release, the microcapsules were spherical and flaky, and the spherical surface was flaky and gathered together in the shape of stearic acid at close range (Figure 3a,c).

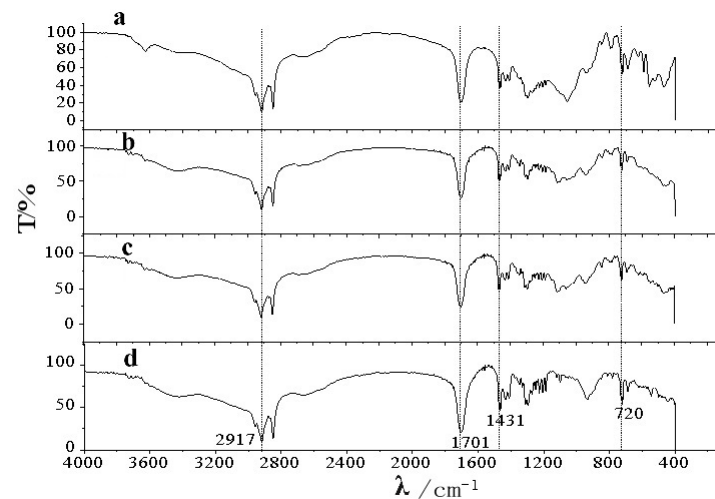


Figure 2. Infrared spectrogram before and after microencapsulation: (a) 1:1 microcapsules, (b) 1:2 microcapsules, (c) 1:3 microcapsules, and (d) stearic acid before microencapsulation.

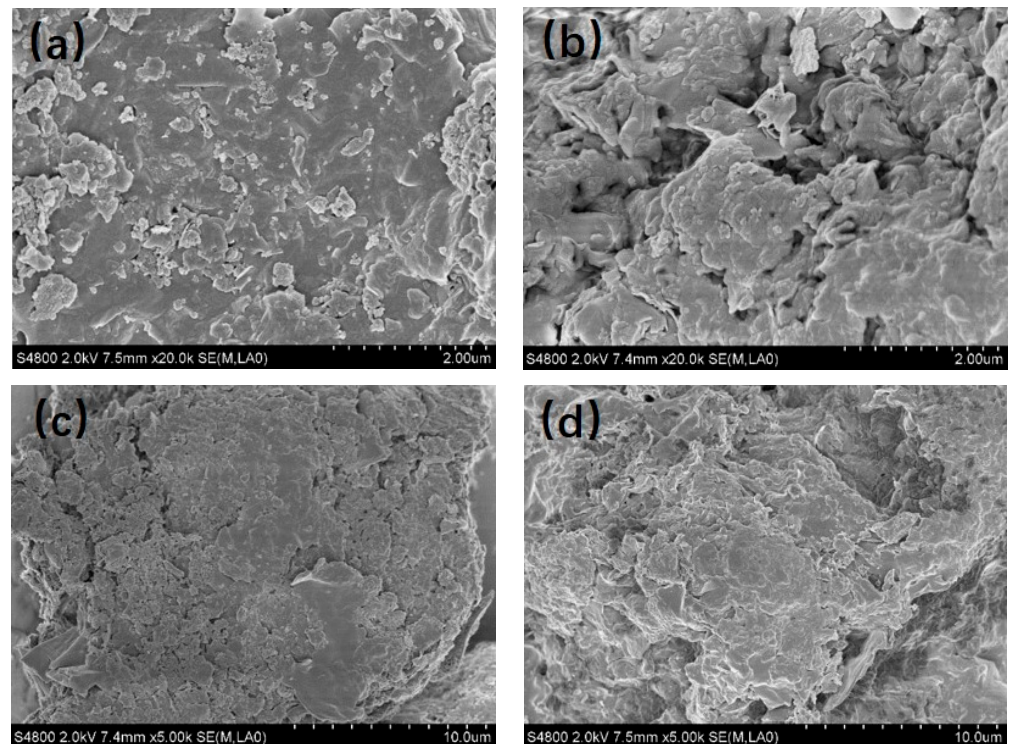


Figure 3. Scanning electron microscopy before and after sustained release of the 1:2 microcapsule. (a) 2 μm before sustained release, (b) 2 μm after sustained release, (c) 10 μm before sustained release, and (d) 10 μm after sustained release.

3.2. Sustained Release Behavior of Potassium Persulfate from the Microcapsules

The sustained release and encapsulation rate were the important factors affecting the performance of the potassium persulfate microcapsules. The sustained release effect of potassium persulfate of microcapsules in deionized water at 25 °C is shown in Figure 4, and it can be seen that the release rate of potassium persulfate gradually increased with the increase in time, and the release rate was close to 60% after 48 h. However, the release rate limits were different in different periods, in which the first 1 h was a rapid release stage and then gradually slowed down after 1 h. Similar results also were detected by Yang [49] and Li [50]. The reason was that some potassium persulfate molecules were been

completely encapsulated by stearic acid in microcapsules, but some potassium persulfate molecules may not have completely encapsulated by stearic acid on the surface of the microcapsules. Potassium persulfate, which was not completely packaged in the surface of the microcapsules, was easy to contact with soil solution, and it was first dissolved in water. So, the release rate increased fast at first, and the first 1 h was a rapid release stage. Potassium persulfate, which was completely packaged in microcapsules, needed to be released through the void formed by the coating layer material or the dissolution of potassium persulfate on the surface. The deeper the potassium persulfate, the greater the pore resistance, so the smaller the diffusion speed [51]. At the same time, it can be seen that the release speed of potassium persulfate also gradually decreases as time goes on. The sustained-release performance of microcapsules was simulated with the kinetic model $Q = kt^n$, where Q is the release rate, K is the release constant, T is the release time (h), and N is the release order [7]. The kinetic equation parameters are shown in Table 1. It indicated that the release rate will reach approximately 90% after 6.8 days in theory. Compared with previous studies on persulfate [52–54], in which reactions usually last for a few minutes or hours, the potassium persulfate microcapsules had a good sustained-release effect in this study.

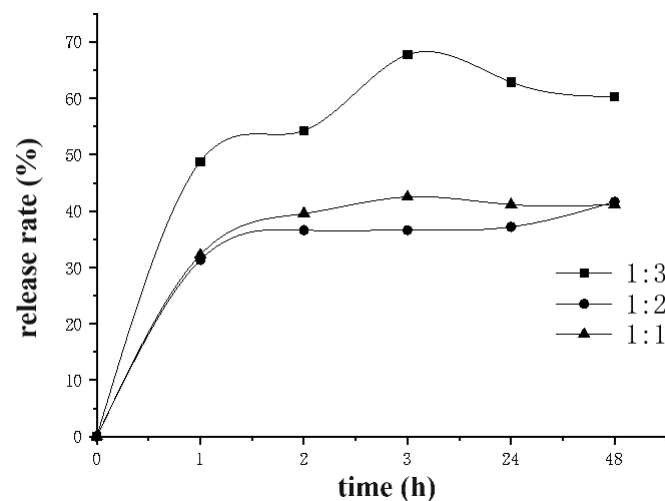


Figure 4. Release curves of potassium persulfate microcapsules.

Table 1. Dynamic simulation of sustained-release performance of microcapsules.

Ratio of Core to Wall (Mass Ratio)	Kinetic Equation	R^2	Time (50% Release Rate)/d	Time (90% Release Rate)/d
1:3	$Q = 5.5471 \cdot t^{0.458}$	0.9988	5	18.2
1:2	$Q = 7.2911 \cdot t^{0.492}$	0.9997	2.1	6.8
1:1	$Q = 9.2343 \cdot t^{0.4761}$	0.9973	1.4	4.9

SEM was used to analyze the sustained release behavior of the microcapsules. Before release, the outer surface was smooth with few concave and convex surfaces and few cracks and holes (Figure 3a,c). After release, the outer surface of the microcapsule spheres diffused [55], and obvious cracks and holes appeared (Figure 3b,d). It was observed at close range that the flaky substances separated from each other, which made potassium persulfate gradually release from the gaps, thus achieving the effect of slow release. It may be the release technique of the potassium persulfate in the deep potassium persulfate microcapsules.

3.3. Degradation of PAH-Contaminated Soil by Microcapsule

3.3.1. Degradation Effect of PAHs

The degradation effect of PAHs remediated by microcapsules in soil is shown in Figure 5. The results in Figure 6 showed that potassium persulfate in microcapsules was gradually released with the extension of reaction time, and the degradation rate of PAHs gradually increased. The degradation rate of PAHs in soil reached 53.6% after 72 h of reaction. Compared with previous research [56], the results of this study showed that the slow-release effect of potassium persulfate wrapped by stearic acid had a good slow-release effect, and the degradation rate of PAHs gradually increased with the slow release of potassium persulfate from microcapsules.

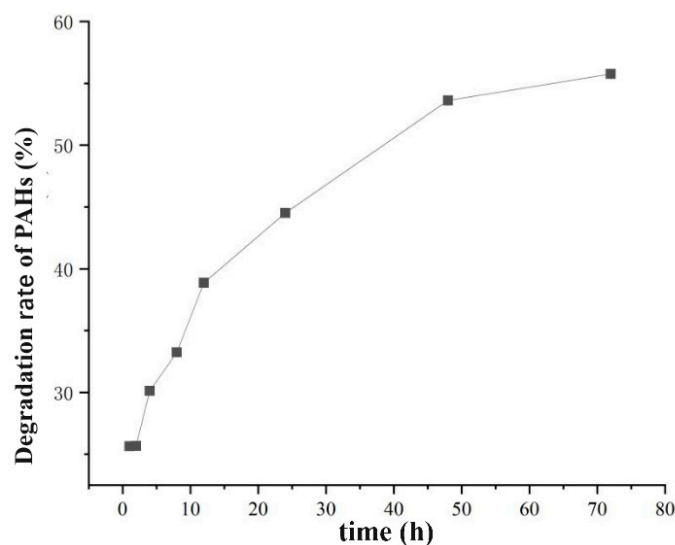


Figure 5. Degradation rate of PAHs in soil by potassium persulfate microcapsules.

3.3.2. Degradation Mechanism of Potassium Persulfate Microcapsules

Radical probe compounds, including ethanol, nitrobenzene, and hexachloromethane, were used to analyze the reaction mechanism of the potassium persulfate microcapsules in this study, and the results are shown in Figure 6. The results showed that the degradation rate of low-ring PAHs and high-ring PAHs after adding ethanol quencher significantly reduced compared with the degradation effect of PAHs in deionized water (Figure 6a,b), and they were only 4.9% and 2.8%. It meant that the microcapsules released potassium persulfate in deionized water and activated under the catalysis of Fe^{2+} , but most of the activated radicals of $\text{SO}_4^{\cdot-}$ and $\cdot\text{OH}$ quenched with ethanol firstly, resulting in radicals consumed and PAHs not being degraded. It showed that the activated radicals of $\text{SO}_4^{\cdot-}$ and $\cdot\text{OH}$ played the main roles in the degradation of PAHs using potassium persulfate microcapsules, and that had been proven by some research when persulfate was acted by metal [23,57,58]. Moreover, the degradation rate of low-ring PAHs is higher than that of high-ring PAHs, so it can be analyzed that the degradation rate of the low ring is faster than that of the high ring in the degradation process of PAHs, and the structure of the high ring is more stable than that of the low ring.

The degradation rate of PAHs after adding nitrobenzene to remove $\cdot\text{OH}$ is shown in Figure 6c. The degradation rates of low-ring PAHs and high-ring PAHs were 60.7% and 31.6% after 5 min reaction, which decreased by 4.3% and 5.2% compared with the blank sample. When the reaction reached 480 min, the degradation rates of low-ring and high-ring were 80.7% and 44%, respectively, which decreased by 10.4% and 24.1% compared with the degradation rate without any free radical quencher. The main reason is that $\cdot\text{OH}$ was quenched by nitrobenzene. The results in Figure 6c suggested that $\text{SO}_4^{\cdot-}$ played a major role in the degradation of PAHs by potassium persulfate microcapsules, and $\cdot\text{OH}$ also played an auxiliary role, particularly in high-ring polycyclic aromatic hydrocarbons.

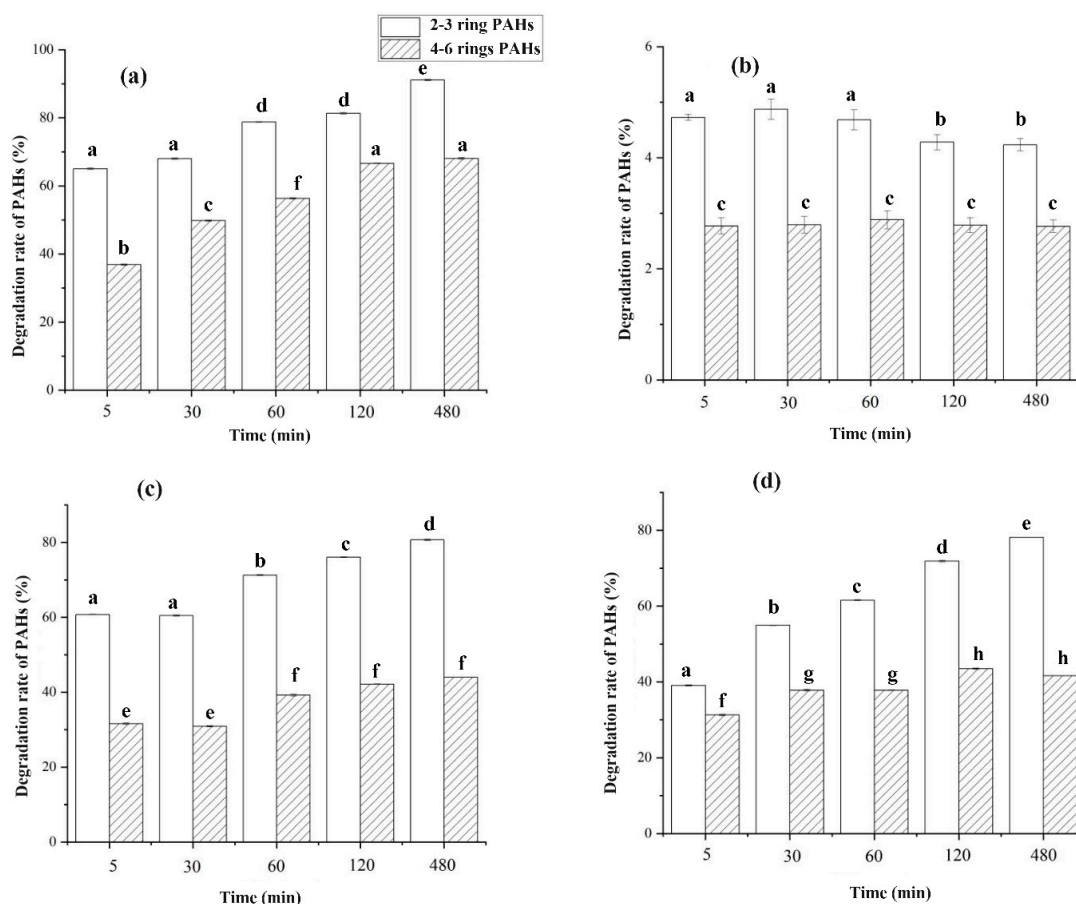


Figure 6. Degradation mechanism study on PAHs by potassium persulfate microcapsules. (a) Degradation effect of PAHs in deionized water, (b) effects of removing free radicals, (c) effect of removing $\cdot\text{OH}$, and (d) effects of removing reducing substances. The different letters indicate statistical differences between the groups (one-way ANOVA test) and represent a 5% significance level.

The degradation rate of PAHs after removing reducing substances by adding hexachloroethane is shown in Figure 6d. The results in Figure 6d showed that the degradation rate of low-ring and high-ring PAHs was only 39.1% and 31.3% after a 5 min reaction, which was 25.9% and 5.5% lower than that without adding a free radical probe reagent. The degradation rates of low-ring and high-ring PAHs were 78.1% and 41.6%, respectively, after 480 min reaction, and they were reduced by 13% and 26.5% compared with the blank sample. The results showed that the reducing substances produced in the system also played an auxiliary role in the degradation of PAHs due to promoting the generation of $\text{SO}_4^{\cdot-}$ and $\cdot\text{OH}$ radicals. The results also showed that with the prolongation of reaction time, the influence of reducing substances on low-ring PAHs gradually decreased, while the influence on high-ring PAHs gradually increased.

To sum up, the free radicals produced from potassium persulfate microcapsules activated by Fe^{2+} were the main reasons to degrade PAHs. During the free radicals, $\text{SO}_4^{\cdot-}$ played the most important major role in the degradation of PAHs by potassium persulfate microcapsules activated by Fe^{2+} , followed by $\cdot\text{OH}$, and the reducing substances also played an auxiliary role.

3.3.3. Effects on Environment After Degradation by Microcapsule

As usual, there were some effects on the environment after the degradation of PAH-contaminated soil. So, the change in pH value in soil, the seed germination rate, and the bacteria quantity in soil after degradation by potassium persulfate microcapsules were detected, and they were used to assess the effects on the environment after degradation

by microcapsules (Figure 7). The results of Figure 7a showed that the soil pH slightly decreased from 6.8 to 6.4 after being degraded by microcapsules, but the changes were not significant ($p > 0.05$). The germination rate of ryegrass seeds was only 42.5% and increased to 97.5% after treatment (Figure 7b). It showed that PAHs had significant effects on the germination rate of ryegrass seeds, which had been proved in previous studies [59], and it suggested that the toxic effect of soil on plants reduced significantly after treatment.

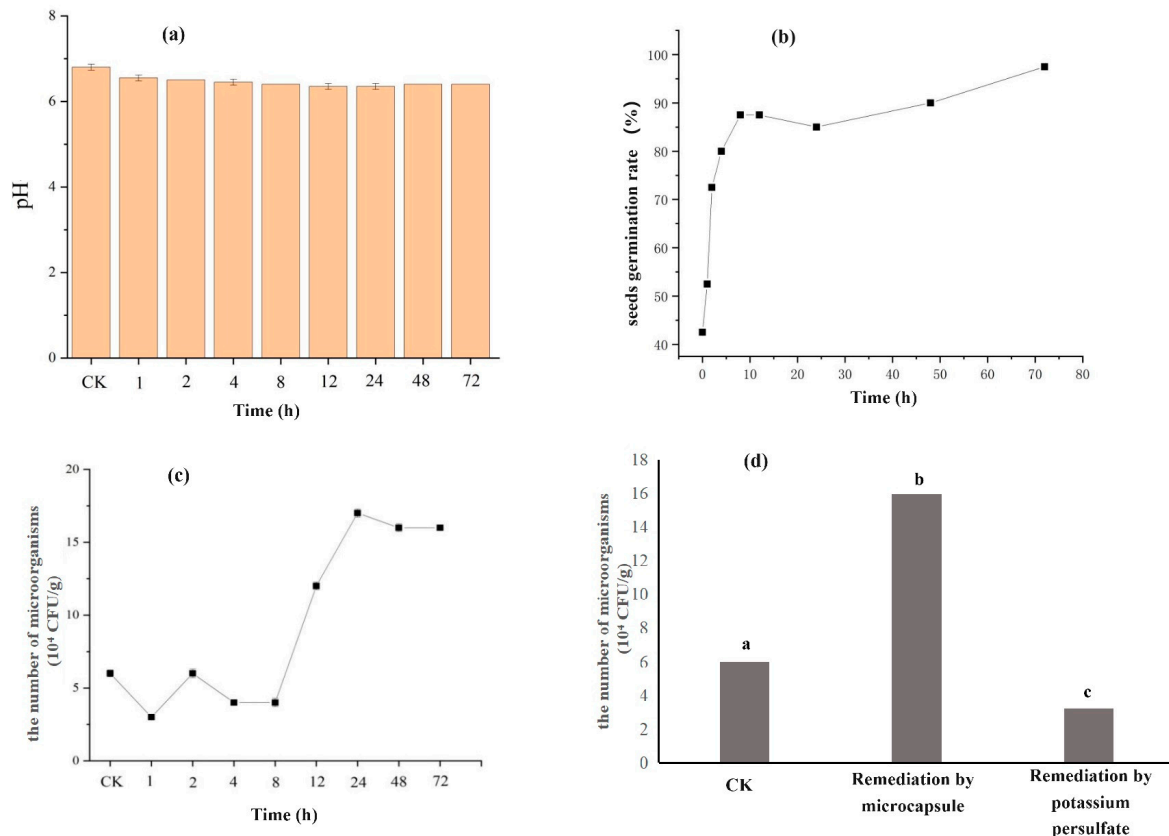


Figure 7. Effects on environments after degradation by microcapsule. (a) Soil pH, (b) seed germination rate, (c) the number of microorganisms in the soil with time, and (d) a comparison of the number of microorganisms in the soil during different treatments. The different letters indicate statistical differences between the groups (one-way ANOVA test) and represent a 5% significance level.

The number of bacteria was enumerated using the most-probable-number methods [60], and the changes in bacteria quantity in soil are shown in Figure 7c. It can be seen that the number of bacteria without microcapsule treatment was 6×10^4 CFU/g. After treatment, the number of bacteria in the soil shows a downward trend and then increases with the extension of reaction time. After 72 h, the number of bacteria reached 16×10^4 CFU/g. That is related to the slow release of potassium persulfate in the microcapsules. PAHs in soil were degraded by potassium persulfate, and it would decrease toxicity on microorganisms. Stearic acid, the wall material of potassium persulfate microcapsules, was used as a carbon source by microorganisms in the soil, which provided the material basis for the growth of microorganisms and increased the number of bacteria in the soil. Meanwhile, the repair process of potassium persulfate microcapsules was more moderate, and the impact on the soil environment was less compared to potassium persulfate. So, the number of microorganisms was significantly higher in the remediation of potassium persulfate microcapsule than potassium persulfate (Figure 7d).

Combined with the above results, the potassium persulfate microcapsules were an oxidation system with little effect on the number of soil microorganisms and a good removal effect of PAHs. It not only degraded PAHs in the soil but also had less effect on

the environment, and it even promoted the growth and development of microorganisms and increased the germination rate of seeds.

4. Conclusions

In summary, this work reported that microencapsulation technology was used to amend potassium persulfate in the remediation of PAHs contaminated soil, in which stearic acid was used to wrap potassium persulfate. The potassium persulfate microcapsules were provided with a good sustained-release effect, and about 60% potassium persulfate was released from microcapsules after 48 h. Based on XRD and the infrared spectrum, the results suggested that no chemical reaction occurred between stearic acid and potassium persulfate. Meanwhile, the degradation mechanism was also discussed, and the results showed that $\text{SO}_4^{\cdot -}$ played the most important major role in the degradation of PAHs, followed by $\cdot\text{OH}$, and the reducing substances also played an auxiliary role. The potassium persulfate microcapsules had a good removal effect of PAHs in soil (53.6% after 72 h), and it had a lower effect on the environment, which was beneficial for subsequent bioremediation. Therefore, this research provided an environment-friendly oxidation system (potassium persulfate microcapsules), and it has broad application prospects.

Author Contributions: Conceived and designed the experiments: H.W. (Hao Wu) and H.W. (Hui Wang). Performed the experiments: H.W. (Hao Wu), Y.W. and X.W. Analyzed the data: H.W. (Hui Wang), and Y.Y. Wrote the paper: H.W. (Hao Wu) and H.W. (Hui Wang). Validation: L.S. All authors have read and agreed to the published version of the manuscript.

Funding: This research was funded by the Open Project Program of Engineering Research Center of Groundwater Pollution Control and Remediation, Ministry of Education of China (GW202309), and the funding project of Northeast Geological S&T Innovation Center of China Geological Survey (No. QCJJ2023-39).

Data Availability Statement: The data presented in this study are available on request from the corresponding author. The data are not publicly available due to confidentiality reasons.

Acknowledgments: The authors thank the staff of Key Laboratory of Regional Environmental and Eco-Remediation, Ministry of Education, Shenyang University for their support during field sampling, logistics, and laboratory analysis.

Conflicts of Interest: The authors declare no competing financial interests.

References

1. Yan, Z.; Gu, Y.; Wang, X.; Hu, Y.; Li, X. Degradation of aniline by ferrous ions activated persulfate: Impacts, mechanisms, and by-products. *Chemosphere* **2020**, *268*, 129237. [PubMed]
2. Liao, X.; Zhao, D.; Yan, X.; Huling, S.G. Identification of persulfate oxidation products of polycyclic aromatic hydrocarbon during remediation of contaminated soil. *J. Hazard. Mater.* **2014**, *276*, 26–34. [PubMed]
3. Kronholm, J.; Desbands, B.; Hartonen, K.; Riekkola, M.L. Environmentally friendly laboratory-scale remediation of PAH-contaminated soil by using pressurized hot water extraction coupled with pressurized hot water oxidation. *Green Chem.* **2002**, *4*, 213–219.
4. Ojinnaka, C.M.; Osuji, L.C.; Achugasim, O. Remediation of hydrocarbons in crude oil-contaminated soils using Fenton's reagent. *Environ. Monit. Assess.* **2012**, *184*, 6527–6540. [PubMed]
5. Esmaeili, A.; Knox, O.; Juhasz, A.; Wilson, S.C. Advancing prediction of polycyclic aromatic hydrocarbon bioaccumulation in plants for historically contaminated soils using *Lolium multiflorum* and simple chemical in-vitro methodologies. *Sci. Total Environ.* **2021**, *772*, 144783.
6. Li, W.; Orozco, R.; Camargos, N.; Liu, H. Mechanisms on the Impacts of Alkalinity, pH, and Chloride on Persulfate-Based Groundwater Remediation. *Environ. Sci. Technol.* **2017**, *51*, 3948–3959.
7. Zhang, J.; Li, Y.F.; Li, M. Experimental Investigation on Removal Efficiency of Reactive Red X-3B in Dye Wastewater by Potassium Ferrate. *Liaoning Chem. Ind.* **2011**, *40*, 120–122. (In Chinese)
8. Cavanagh, B.A.; Johnson, P.C.; Daniels, E.J. Reduction of diffusive contaminant emissions from a dissolved source in a lower permeability layer by sodium persulfate treatment. *Environ. Sci. Technol.* **2014**, *48*, 14582–14589.
9. Gul, S.; Miano, T.F.; Mujeeb, A.; Chachar, M.; Majeedano, M.I.; Murtaza, G.; Ahmed, W.; Khanzada, Y.A.; Ansari, M. Advancements in nutraceutical delivery: Integrating nanotechnology and microencapsulation for enhanced efficacy and bioavailability. *Matrix Sci. Pharma* **2024**, *8*, 1–6. [CrossRef]

10. Paes, F.E.R.; Sabino, L.B.D.S.; da Silva, L.M.R.; da Silva, I.J.; Ricardo, N.M.P.S.; de Brito, D.H.A.; de Menezes, F.L.; de Figueiredo, R.W. Anthocyanins extracted from Jamelon fruits (*Syzygium cumini* L.): Effect of microencapsulation on the properties and bioaccessibility. *S. Afr. J. Bot.* **2024**, *166*, 423–431.
11. Shen, J.; Zhang, M.; Yang, C. Microencapsulation of ginger essential oil using mung bean protein isolate-chitosan complex coacervates: Application in the preservation of crab meatballs and the prediction of shelf life. *Food Chem.* **2024**, *449*, 139263. [[PubMed](#)]
12. Davis, E.; Walker, T.R.; Adams, M.; Willis, R. Characterization of polycyclic aromatic hydrocarbons (PAHs) in small craft harbour (SCH) sediments in Nova Scotia, Canada. *Mar. Pollut. Bull.* **2018**, *137*, 285–294. [[PubMed](#)]
13. Li, M.; Yin, H.; Zhu, M.; Yu, Y.; Lu, G.; Dang, Z. Co-metabolic biochar-promoted biodegradation of mixed PAHs by highly efficient microbial consortium QY1. *J. Environ. Sci.* **2021**, *107*, 65–76.
14. Saleh, S.M.; Farhan, F.J.; Khwedem, A.A.; Al-Saad, H.T.; Zahraal-Hello, A. Assessment of polycyclic aromatic hydrocarbons (PAHs) in water and sediments at south part of Alhammer Marsh, southern Iraq. *Poll Res.* **2021**, *40*, 79–87.
15. Dhar, K.; Panneerselvan, L.; Venkateswarlu, K.; Megharaj, M. Efficient bioremediation of PAHs-contaminated soils by a methylo-trophic enrichment culture. *Biodegradation* **2022**, *33*, 575–591. [[PubMed](#)]
16. Chen, T.; Dong, Y.; Huang, W.; Ma, Y. Dynamics of microbial community and functional genes during bioremediation of PAHs-contaminated soil by two biostimulants. *Biochem. Eng. J.* **2024**, *208*, 109356.
17. Wang, C.P.; Li, J.; Jiang, Y.; Zhang, Z.Y. Enhanced bioremediation of field agricultural soils contaminated with PAHs and OCPs. *Int. J. Environ. Res.* **2014**, *8*, 1271–1278.
18. Davis, E.; Walker, T.R.; Adams, M.; Willis, R. Estimating PAH sources in harbor sediments using diagnostic ratios. *Rem. J.* **2019**, *29*, 51–62.
19. Davis, E.; Walker, T.R.; Adams, M.; Willis, R.; Norris, G.A.; Henry, R.C. Source apportionment of polycyclic aromatic hydrocarbons (PAHs) in small craft harbor (SCH) surficial sediments in Nova Scotia, Canada. *Sci. Total Environ.* **2019**, *691*, 528–537.
20. Han, X.M.; Liu, Y.R.; Zheng, Y.M.; Zhang, X.X.; He, J.Z. Response of bacterial *pdo1*, *nah*, and *C12O* genes to aged soil PAH pollution in a coke factory area. *Environ. Sci. Pollut. Res.* **2014**, *21*, 9754–9763.
21. Sun, J.; Pan, L.; Tsang, D.C.W.; Zhan, Y.; Zhu, L.; Li, X. Organic contamination and remediation in the agricultural soils of China: A critical review. *Sci. Total Environ.* **2018**, *615*, 724–740. [[PubMed](#)]
22. Stamatelopoulou, A.; Dasopoulou, M.; Bairachtari, K.; Karavoltso, S.; Maggos, T. Contamination and Potential Risk Assessment of Polycyclic Aromatic Hydrocarbons (PAHs) and heavy metals in house settled dust collected from residences of young children. *Appl. Sci.* **2021**, *11*, 1479. [[CrossRef](#)]
23. Wang, Y.; Nie, M.; Diwu, Z.; Chang, F.; Nie, H.; Zhang, B.; Bai, X.; Yin, Q. Toxicity evaluation of the metabolites derived from the degradation of phenanthrene by one of a soil ubiquitous PAHs-degrading strain *Rhodococcus qingshengii* FF. *J. Hazard. Mater.* **2021**, *415*, 125657. [[CrossRef](#)] [[PubMed](#)]
24. Ma, T.T.; Luo, Y.M.; Christie, P.; Teng, Y.; Liu, W.X. Removal of phthalic esters from contaminated soil using different cropping systems: A field study. *Eur. J. Soil Biol.* **2012**, *50*, 76–82. [[CrossRef](#)]
25. Wang, H.; Zhao, Y.; Muhammad, A.; Liu, C.; Luo, Q.; Wu, H.; Wang, X.; Zheng, X.; Wang, K.; Du, Y. Influence of celery on the remediation of PAHs contaminated farm soil. *Soil Sediment Contam.* **2019**, *28*, 200–212. [[CrossRef](#)]
26. Zheng, X.; Ding, H.; Xu, X.; Liang, B.; Liu, X.; Zhao, D.; Sun, L. In situ phytoremediation of polycyclic aromatic hydrocarbon-contaminated agricultural greenhouse soil using celery. *Environ. Technol.* **2021**, *42*, 3329–3337. [[CrossRef](#)]
27. Falciglia, P.P.; De Guidi, G.; Catalfo, A.; Vagliasindi, F.G.A. Remediation of soils contaminated with PAHs and nitro-PAHs using microwave irradiation. *Chem. Eng. J.* **2016**, *296*, 162–172. [[CrossRef](#)]
28. Jia, J.L.; Wang, B.B.; Wu, Y.; Niu, Z.; Ma, X.Y.; Yu, Y.; Hou, P. Environmental risk controllability and management of VOCs during remediation of contaminated sites. *Soil Sed. Contam.* **2016**, *25*, 13–25. [[CrossRef](#)]
29. Lim, M.W.; Von Lau, E.; Poh, P.E. A comprehensive guide of remediation technologies for oil contaminated soil—Present works and future directions. *Mar. Pollut. Bull.* **2016**, *109*, 14–45.
30. Kolthoff, I.M.; Medalia, A.I.; Raaen, H.P. The Reaction between Ferrous Iron and Peroxides. IV. Reaction with Potassium Persulfate1a. *J. Am. Chem. Soc.* **1951**, *73*, 1733–1739. [[CrossRef](#)]
31. Li, C.Q.; Zou, Y.C.; Jia, X.N. Research progress in activation methods of persulfate and degradation mechanism of organic pollutants by persulfate advanced oxidation process. *Chem. Bioeng.* **2022**, *39*, 1–6, 27. (In Chinese)
32. Tao, S.; Wang, W.T.; Liu, W.X.; Zuo, Q.; Wang, X.L.; Wang, R.; Wang, B.; Shen, G.F.; Yang, Y.H.; He, J.S. Polycyclic aromatic hydrocarbons and organochlorine pesticides in surface soils from the Qinghai-Tibetan plateau. *J. Environ. Monit.* **2011**, *13*, 175–181. [[CrossRef](#)] [[PubMed](#)]
33. Fan, F.Q.; Dou, J.F.; Ding, A.Z.; Chen, H.Y.; Du, Y.C. Measurement of high molecular weight polycyclic aromatic hydrocarbons in soil using ultrasonic extraction and HPLC. *J. Beijing Norm. Univ. (Nat. Sci.)* **2011**, *47*, 296–299.
34. Shi, Z.; Tao, S.; Pan, B.; Fan, W.; He, X.C.; Zuo, Q.; Wu, S.P.; Li, B.G.; Cao, J.; Liu, W.X.; et al. Contamination of rivers in Tianjin, China by polycyclic aromatic hydrocarbons. *Environ. Pollut.* **2005**, *134*, 97–111. [[CrossRef](#)]
35. Zhang, H.L.; Sun, L.N.; Sun, T.H.; Li, H.Y.; Luo, Q. Spatial distribution and seasonal variation of polycyclic aromatic hydrocarbons (PAHs) contaminations in surface water from the Hun River, Northeast China. *Environ. Monit. Assess.* **2013**, *185*, 1451–1462. [[CrossRef](#)]

36. Wang, X.; Sun, L.; Wang, H.; Wu, H.; Chen, S.; Zheng, X. Surfactant-enhanced bioremediation of DDTs and PAHs in contaminated farmland soil. *Environ. Technol.* **2018**, *39*, 1733–1744. [[CrossRef](#)]
37. Li, F.Y.; Xie, Y.; Wang, Y.; Fan, X.J.; Cai, Y.B.; Mei, Y.Y. Improvement of dyes degradation using hydrofluoric acid modified biochar as persulfate activator. *Environ. Pollut. Bioavail.* **2019**, *31*, 32–37. [[CrossRef](#)]
38. Dionysiou, D.; Anipsitakis, G.P. Radical generation by the interaction of transition metals with common oxidants. *Environ. Sci. Technol.* **2004**, *38*, 3705–3712.
39. Liang, C.; Su, H. Identification of Sulfate and Hydroxyl Radicals in Thermally Activated Persulfate. *Ind. Eng. Chem. Res.* **2009**, *48*, 5558–5562. [[CrossRef](#)]
40. Neta, P.; Madhavan, V.; Zemel, H.; Fessenden, R.W. Rate constants and mechanism of reaction of $\text{SO}_4^{\cdot -}$ with aromatic compounds. *J. Am. Chem. Soc.* **1977**, *99*, 163–164. [[CrossRef](#)]
41. Buxton, G.V.; Greenstock, C.L.; Helman, W.P.; Ross, A.B. Critical review of rate constants for reactions of hydrated electrons, hydrogen atoms and hydroxyl radicals ($\cdot\text{OH}/\cdot\text{O}^-$) in aqueous solution. *J. Phys. Chem. Ref. Data* **1988**, *17*, 513–780. [[CrossRef](#)]
42. Teel, A.L.; Ahmad, M.; Watts, R.J. Persulfate activation by naturally occurring trace minerals. *J. Hazard. Mater.* **2011**, *196*, 153–159. [[CrossRef](#)] [[PubMed](#)]
43. Ye, M.; Yuan, B.; Lan, H.; Fu, M. Preparation and characterization of embedded potassium ferrate for controlled release. *Chin. High Technol. Lett.* **2008**, *18*, 201–205. (In Chinese)
44. Li, D.; Wu, H.; Huang, W.; Guo, L.; Dou, H. Microcapsule of sweet orange essential oil encapsulated in beta-cyclodextrin improves the release behaviours in vitro and in vivo. *Eur. J. Lipid Sci. Technol.* **2018**, *120*, 1700521. [[CrossRef](#)]
45. Ma, X.C.; Liu, Y.J.; Liu, H.; Li, L.Z. Preparation and thermal physical properties of paraffin@TiO₂/CNTs composite phase change materials. *J. Zhejiang Univ. Technol.* **2020**, *48*, 85–89. (In Chinese)
46. Xia, Z.K.; Lian, S.X.; Yin, D.L.; Li, C.Z.; Zhang, H.J. Stearic acid coating for CaS: Eu Phosphor. *J. Nat. Sci. Hunan Norm. Univ.* **2007**, *30*, 64–67. (In Chinese)
47. Jiang, Z.M.; Bai, L.N.; Yang, N.; Feng, Z.B.; Tian, B. Stability of β -carotene microcapsules with Maillard reaction products derived from whey protein isolate and galactose as coating materials. *J. Zhejiang Univ.-Sci. B (Biomed. Biotechnol.)* **2017**, *10*, 94–104. (In Chinese) [[CrossRef](#)]
48. Lashgari, S.; Mahdavian, A.R.; Arabi, H.; Ambrogi, V.; Marturano, V. Preparation of acrylic PCM microcapsules with dual responsivity to temperature and magnetic field changes. *Eur. Polym. J.* **2018**, *101*, 18–28. [[CrossRef](#)]
49. Yang, Y.; Zhang, Q.; Peng, C.; Wu, B.; Xu, J.; Ma, F.; Gu, B. Sustained-Release of Sodium Persulfate Composite and Degradation of 2020, 2,4-Dinitrotoluene. *Res. Environ. Sci* **2020**, *33*, 769–776. (In Chinese)
50. Li, Q.G.; Yan, X.M.; Chen, J.L.; Shu, X.G.; Jia, P.Y.; Liang, X.J. Preparation and characterization of potassium monopersulfate/ethyl cellulose microcapsules and their sustained release performance. *J. Renew. Mater.* **2021**, *9*, 1673–1684. [[CrossRef](#)]
51. Ao, Z.; Xu, R.; Xie, X. Synthesis and properties of persulfate microcapsule slow-released materials. *Saf. Environ. Eng.* **2018**, *25*, 25–29, 35. (In Chinese)
52. Gao, S.X.; Zhang, N.; Chen, L. Degradation of tetracycline by activated peroxodisulfate using a sulfur-modified iron-based material. *Water Sci. Technol. J. Int. Assoc. Water Pollut. Res.* **2023**, *87*, 2905–2916. [[CrossRef](#)] [[PubMed](#)]
53. Xiao, S.; Zhang, L.N.; Zhou, L.A.; Zhong, H.; Brusseau, M.L.; Li, Y.; Wang, Y.K.; Liu, G.S.; Zhang, J.T. The long-term effect of Fe₃O₄ in activating persulfate to degrade refractory organic contaminants for groundwater remediation. *Chem. Eng. J.* **2024**, *482*, 148801. [[CrossRef](#)]
54. Zhang, M.; Feng, M.Y.; Xu, Z.Q.; Li, J.N.; Peng, C. Electrokinetically-delivered persulfate coupled with thermal conductive heating for remediation of petroleum hydrocarbons contaminated low permeability soil. *Chemosphere* **2024**, *356*, 141914. [[CrossRef](#)] [[PubMed](#)]
55. Mu, R.J.; Yuan, Y.; Wang, L.; Ni, Y.; Li, M.; Chen, H.; Pang, J. Microencapsulation of Lactobacillus acidophilus with konjac glucomannan hydrogel. *Food Hydrocoll.* **2017**, *76*, 42–48. [[CrossRef](#)]
56. Xu, Y.; Zhang, H.; Wei, Z.; Zhang, X.; Zhao, C.; Li, H.; Hu, F.; Xu, L. Effects of sulfate radical advanced oxidation technology on PAHs remediation in contaminated sites. *Soils* **2020**, *52*, 532–538. (In Chinese)
57. Desalegn, B.; Megharaj, M.; Chen, Z.; Naidu, R. Green mango peel-nanozerovalent iron activated persulfate oxidation of petroleum hydrocarbons in oil sludge contaminated soil. *Environ. Technol. Innov.* **2018**, *11*, 142–152. [[CrossRef](#)]
58. Wan, Z.; Sun, Y.; Tsang, D.C.W.; Yu, I.K.M.; Fan, J.J.; Clark, J.H.; Zhou, Y.Y.; Cao, X.D.; Gao, B.; Ok, Y.S. A sustainable biochar catalyst synergized with copper heteroatoms and CO₂ for singlet oxygenation and electron transfer routes. *Green Chem.* **2019**, *21*, 4800–4814. [[CrossRef](#)]
59. Wang, C.; Li, X.; Dong, F.; Wei, L.; Yang, L.; Sun, C.; Lin, A. Changes in polyaromatic hydrocarbons contaminated soil properties and phytotoxicity under chemical oxidation. *J. Beijing Univ. Chem. Technol. (Nat. Sci.)* **2012**, *39*, 95–100. (In Chinese)
60. Wrenn, B.A. Venosa AD. Selective enumeration of aromatic and aliphatic hydrocarbon degrading bacteria by a most-probable-number procedure. *Can. J. Microbiol.* **1996**, *42*, 252–258. [[CrossRef](#)]

Disclaimer/Publisher’s Note: The statements, opinions and data contained in all publications are solely those of the individual author(s) and contributor(s) and not of MDPI and/or the editor(s). MDPI and/or the editor(s) disclaim responsibility for any injury to people or property resulting from any ideas, methods, instructions or products referred to in the content.